

FRACTURE OF A MATERIAL COMPRESSED ALONG TWO CLOSELY SPACED PENNY-SHAPED CRACKS

M. V. Dovzhik

A nonclassical problem of fracture mechanics for a body with two closely spaced parallel coaxial penny-shaped cracks is solved. In the case of equal roots of the characteristic equations, an axisymmetric problem is considered. Materials with harmonic and Bartenev–Khazanovich potentials are analyzed numerically. The numerical results are presented in the form of tables and graphs and analyzed

Keywords: two parallel cracks, compression, critical stress

Introduction. When the forces acting on a body with two parallel penny-shaped cracks are parallel to the crack plane, the stress intensity factors predicted by classical fracture mechanics are equal to zero and the Irwin–Griffith failure criteria are inapplicable. When a load acts along the crack plane, use is made of the approach proposed in [2, 3] and used and developed in [4–15]. The failure criterion in this case is local loss of stability near the crack described by the three-dimensional linearized theory of elastic stability [2]. According to this approach, fracture is initiated by local loss of stability near cracks, and the critical compressive loads are determined by solving the appropriate eigenvalue problems using the three-dimensional linearized theory of stability of deformable bodies.

In [4–16], the critical compressive strains and stresses were determined for different arrangements of interacting cracks and for different distances between the cracks (between the crack and the free surface). In [4, 9, 12], for example, the relationship between β and the critical compressive strain (stress) was established for two parallel penny-shaped cracks (Fig. 1: $\beta = ha^{-1}$, where $2h$ is the distance between the cracks; a is the crack radius) and potentials of different types. Also of great interest is the behavior of the critical parameters in asymptotic cases ($\beta \rightarrow \infty$, $\beta \rightarrow 0$). In the case $\beta \rightarrow \infty$, such asymptotics was obtained in [4]. The critical compressive stresses tend to the level corresponding to a single crack.

When $\beta \rightarrow 0$, the situation is more involved because the available numerical methods encounter insuperable difficulties associated with the ill-conditioning of the matrices at small β (the determinant is close to zero, and the critical points are determined by equating the determinant to zero). Approximate design models [17] cannot also be used to analyze this issue because the boundary conditions for the thin plate isolated by the cracks have to range from simple support to clamping, which leads to a four-fold difference in results for a rectangular plate under uniaxial compression and to a 3.5-fold difference for a circular plate under uniform biaxial compression. However, this issue is of both theoretical and practical interest when there are thin interlayers formed after spraying, thermal shock, etc.

Note that the results for a near-surface crack [7, 10] and two parallel cracks in the case of unequal roots of the characteristic equation [11] are similar in asymptotic behavior to the results for a clamped thin circular plate between a crack and the free surface or between two cracks.

Since it is difficult to analytically solve such problems as $\beta \rightarrow 0$, we used a Wolfram Mathematica package for symbolic mathematics for that purpose for arbitrary β . This allowed using the method for solving integral equations proposed in [7, 10, 11] to obtain a solution for short distances between the cracks in the case of equal roots of the characteristic equation.

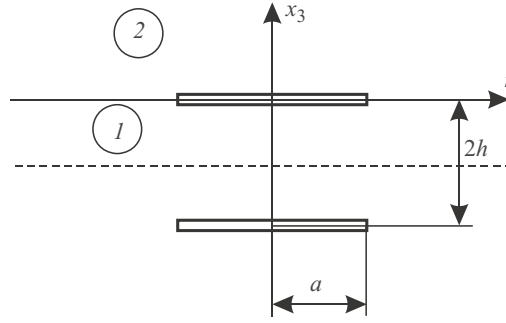


Fig. 1

1. Problem Formulation and Generalized Solution. Consider two parallel penny-shaped cracks of radius a located in the planes $x_3 = 0$ and $x_3 = -2h$ and centered on the Ox_3 -axis (Fig. 1). The prestresses acting along the cracks are induced by biaxial tension/compression. The crack faces are free from stresses. Uniform compression induces a homogeneous subcritical state in the infinite body:

$$S_{33}^0 = 0, \quad S_{11}^0 = S_{22}^0 \neq 0, \quad u_m^0 = \delta_{jm} (\lambda_j - 1)x_j \quad (\lambda_1 = \lambda_2 \neq \lambda_3, \lambda_j = \text{const}),$$

where λ_j are the elongations along the axes; x_j are the Lagrange coordinates that coincide with the Cartesian coordinates before deformation; S_{ij}^0 are the components of the symmetric stress tensor; u_j^0 are the displacements corresponding to the prestresses S_{ij}^0 .

The boundary conditions of the linearized problem are

$$t_{33} = 0, \quad t_{3r} = 0, \quad x_3 = (0)_{\pm}, \quad t_{33} = 0, \quad t_{3r} = 0, \quad x_3 = (-2h)_{\pm} \quad (0 \leq r < a), \quad (1.1)$$

where the indices “+” and “-” refer to the crack faces; (r, θ, x_3) are the cylindrical coordinates transformed from the Cartesian coordinates x_j ; t_{ij} is the asymmetric Kirchhoff stress tensor.

In the case of unequal roots of the characteristic equation [4], the linearized equations of the axisymmetric problem have the following generalized solutions:

$$u_r = -\frac{\partial \varphi}{\partial r} - z_1 \frac{\partial F}{\partial r}, \quad u_3 = (m_1^0 - m_2^0 + 1)(n_1^0)^{-1/2} F - m_1^0 (n_1^0)^{-1/2} \Phi - m_1^0 (n_1^0)^{-1/2} \frac{\partial F}{\partial z_1},$$

$$t_{33} = C_{44}^0 \left\{ (d_1^0 l_1^0 - d_2^0 l_2^0) \frac{\partial F}{\partial z_1} - d_1^0 l_1^0 \frac{\partial \Phi}{\partial z_1} - d_1^0 l_1^0 z_1 \frac{\partial^2 F}{\partial z_1^2} \right\},$$

$$t_{3r} = C_{44}^0 \left\{ (n_1^0)^{-\frac{1}{2}} \frac{\partial}{\partial r} \left[(d_1^0 - d_2^0) F - d_1^0 \Phi - d_1^0 z_1 \frac{\partial F}{\partial z_1} \right] \right\}, \quad (1.2)$$

where $\varphi = -(\varphi_1 + \varphi_2)$, $F = -\partial \varphi_2 / \partial z_1$, $\Phi = \partial \varphi / \partial z_1$ are harmonic functions satisfying the Laplace equation; $z_i = (n_i^0)^{-1/2} x_3$; $C_{44}^0, m_i^0, n_i^0, d_i^0, l_i^0$ depend on the chosen potential and theory of initial deformations.

A body with two penny-shaped cracks can undergo symmetric and bending buckling. In [4] it was shown that bending buckling occurs at lower compressive prestress. Since local buckling near the crack is a failure criterion and the minimum stress at which fracture sets in is of greatest interest, we will deal with bending buckling. Then the boundary conditions for a half-space are

$$t_{33} = 0, \quad t_{3r} = 0, \quad x_3 = (0)_{\pm} \quad (0 \leq r < a), \quad t_{33} = 0, \quad u_r = 0, \quad x_3 = -h \quad (0 \leq r < \infty). \quad (1.3)$$

2. Fredholm Equations. Following [12], we will obtain dual Fredholm equations. Let us partition the half-space $x_3 \geq -h$ into sections 1 ($x_3 \geq 0$) and 2 ($-h \leq x_3 \leq 0$) on which the potential function is represented as the Hankel transform:

$$\begin{aligned} \varphi^{(1)}(r, z_1) &= -\int_0^\infty B(\lambda) e^{-\lambda z_1} J_0(\lambda r) \frac{d\lambda}{\lambda}, & F^{(1)}(r, z_1) &= \int_0^\infty A(\lambda) e^{-\lambda z_1} J_0(\lambda r) d\lambda, \\ \Phi^{(1)}(r, z_1) &= \int_0^\infty B(\lambda) e^{-\lambda z_1} J_0(\lambda r) d\lambda, \\ \varphi^{(2)}(r, z_1) &= \int_0^\infty [D_1(\lambda) \sinh \lambda(z_1 + h_1) + D_2(\lambda) \cosh \lambda(z_1 + h_1)] J_0(\lambda r) \frac{d\lambda}{\lambda + \sinh \lambda h_1}, \\ F^{(2)}(r, z_2) &= \int_0^\infty [C_1(\lambda) + \cosh \lambda(z_1 + h_1) + C_2(\lambda) + \sinh \lambda(z_1 + h_1)] J_0(\lambda r) \frac{d\lambda}{+\sinh \lambda h_1}, \\ \Phi^{(2)}(r, z_1) &= \int_0^\infty [D_1(\lambda) + \cosh \lambda(z_1 + h_1) + D_2(\lambda) + \sinh \lambda(z_1 + h_1)] J_0(\lambda r) \frac{d\lambda}{+\sinh \lambda h_1} \\ & (h_1 = (n_1^0)^{-1/2} h). \end{aligned} \tag{2.1}$$

Following [12], we use (1.3), (1.2), and (2.1) to obtain dual integral equations:

$$\begin{aligned} \int_0^\infty [C_1(\mu_1 \coth \mu_1 - k_1) - D_1] J_0(\lambda r) \lambda d\lambda &= 0 \quad (0 \leq r < a), \\ \int_0^\infty [C_1(\mu_1 - k_2 \coth \mu_1) + D_1 \coth \mu_1] J_0(\lambda r) d\lambda &= \tilde{c} \quad (r < a), \\ \int_0^\infty x_1 J_0(\lambda r) d\lambda = 0, & \quad \int_0^\infty x_2 J_0(\lambda r) \lambda d\lambda = 0 \quad (r > a), \end{aligned} \tag{2.2}$$

where $\tilde{c} = \text{const}$ has units of length; C_2, D_2, A, B are given by

$$\begin{aligned} C_2(\lambda) &= 0, & D_2(\lambda) &= \mu_1 C_1(\lambda), \\ A(\lambda) &= \frac{1}{k} \left[\mu_1 (1 + \coth \mu_1) - k_2 \left(\frac{k_1}{k_2} + \coth \mu_1 \right) \right] C_1(\lambda) + \frac{1}{k} D_1(\lambda) (1 + \coth \mu_1), \\ B(\lambda) &= \frac{k_2}{k} C_1(\lambda) \left[\mu_1 \left(\frac{k_1}{k_2} + \coth \mu_1 \right) - k_1 (1 + \coth \mu_1) \right] + \frac{k_1}{k} D_1(\lambda) \left(\frac{k_1}{k_2} + \coth \mu_1 \right) \end{aligned} \tag{2.3}$$

with

$$\begin{aligned} x_1 &= [(\mu_1 - k_1) C_1 - D_1] (\coth \mu_1 + 1), & x_2 &= [(\mu_1 - k_2) C_1 - D_1] (\coth \mu_1 + 1), \\ \mu_1 &= \lambda h_1, & k_1 &= 1 - \frac{l_2 d_2}{l_1 d_1}, & k_2 &= 1 - \frac{d_2}{d_1}, & k &= k_1 - k_2. \end{aligned} \tag{2.4}$$

Let the solution of the dual integral equations have the form

$$x_1 = \frac{1}{\lambda} \int_0^a \varphi(t)(\cos \lambda t - \cos \lambda a) dt, \quad x_2 = h \int_0^a \psi(t) \cos \lambda t dt. \quad (2.5)$$

Performing transformations and nondimensionalizing the variables and functions, we obtain a system of two Fredholm equations with an additional condition:

$$\begin{aligned} f(\xi) - \frac{1}{\pi k} \int_0^1 M_1(\xi, \eta) f(\eta) d\eta - \frac{2}{\pi k} \int_0^1 N_1(\xi, \eta) g(\eta) d\eta &= 0, \\ g(\xi) - \frac{1}{\pi k} \int_0^1 M_2(\xi, \eta) g(\eta) d\eta - \frac{2}{\pi k} \int_0^1 N_2(\xi, \eta) f(\eta) d\eta + \tilde{C}_1 &= 0, \\ \int_0^1 g(\xi) d\xi = 0 \quad (0 \leq \xi \leq 1, 0 \leq \eta \leq 1), \quad f(\xi) \equiv \varphi(a\xi), \quad g(\xi) \equiv \psi(a\xi), \end{aligned} \quad (2.6)$$

where \tilde{C}_1 is an unknown constant related to the additional condition.

The kernels of the integral equations are given by

$$\begin{aligned} M_1(\xi, \eta) &= R_1(\eta + \xi) - R_1(1 + \xi) + R_1(\eta - \xi) - R_1(1 - \xi), \\ N_1(\xi, \eta) &= S_1(\eta + \xi) + S_1(\eta - \xi), \quad M_2(\xi, \eta) = S_2(\eta + \xi) + S_2(\eta - \xi), \\ N_2(\xi, \eta) &= R_2(\eta + \xi) - R_2(1 + \xi) + R_2(\eta - \xi) - R_2(1 - \xi), \\ R_1(\zeta) &= \beta_1 \frac{\beta_1^2(1+k) + (k-1)\zeta^2}{(\beta_1^2 + \zeta^2)^2}, \quad R_2(\zeta) = \frac{\beta_1}{\beta_1^2 + \zeta^2}, \\ S_1(\zeta) &= \frac{\beta_1^3}{2} \frac{\beta_1^2 - 3\zeta^2}{(\beta_1^2 + \zeta^2)^3}, \quad S_2(\zeta) = \beta_1 \frac{\beta_1^2(1-k) - (k+1)\zeta^2}{(\beta_1^2 + \zeta^2)^2}, \quad \beta_1 = 2(n_1^0)^{-1/2} \beta. \end{aligned} \quad (2.7)$$

3. Procedure of Analysis. The further analysis employs Wolfram Mathematica 7, which is an efficient package for symbolic computation with guaranteed accuracy.

To determine the critical compressive and tensile strains and stresses from the integral equations (2.6), we use a procedure developed in [7] based on the Bubnov–Galerkin method. Let the coordinate functions be power functions. For $N + 1$ coordinate functions, we have

$$f(x) = \sum_{i=0}^N F_i x^i, \quad g(x) = \sum_{i=0}^N G_i x^i. \quad (3.1)$$

Unlike the previous studies [4, 9, 12] where system (2.6) was numerically integrated after the substitution of the coordinate functions, we use Mathematica for analytic evaluation of the integrals for the chosen system of coordinate functions. This allows us to increase the accuracy of computation by excluding the error of numerical integration.

To accelerate the evaluation of integrals, we use an algorithm based on recurrence formulas. Let us introduce the following functions:

$$L(n) = \int_0^1 \frac{x^n}{(a^2 + (x+y)^2)^2} dx, \quad V(n) = \int_0^1 \frac{x^n}{(a^2 + (x-y)^2)^2} dx, \quad (3.2)$$

$$LL(n) = \int_0^1 \frac{x^n}{(a^2 + (x+y)^2)^4} dx, \quad VV(n) = \int_0^1 \frac{x^n}{(a^2 + (x-y)^2)^4} dx. \quad (3.3)$$

We use the following recurrence formulas to evaluate integrals (3.2) and (3.3):

$$\begin{aligned} L(n) &= \frac{1}{n-3} \left(\frac{1}{a^2 + (1+y)^2} - 2y(n-2)L(n-1) - (a^2 + y^2)(n-1)L(n-2) \right) \quad (n \neq 3), \\ V(n) &= \frac{1}{n-3} \left(\frac{1}{a^2 + (1-y)^2} + 2y(n-2)V(n-1) - (a^2 + y^2)(n-1)V(n-2) \right) \quad (n \neq 3), \\ LL(n) &= \frac{1}{n-5} \left(\frac{1}{(a^2 + (1+y)^2)^3} - 2y(n-4)LL(n-1) - (a^2 + y^2)(n-1)LL(n-2) \right) \quad (n \neq 5), \\ VV(n) &= \frac{1}{n-5} \left(\frac{1}{(a^2 + (1-y)^2)^3} + 2y(n-4)VV(n-1) - (a^2 + y^2)(n-1)VV(n-2) \right) \quad (n \neq 5). \end{aligned} \quad (3.4)$$

Having the values of integrals (3.2) for $n = 0, 1, 3$ and (3.3) for $n = 0, 1, 5$ and using the recurrence formulas (3.4), we can evaluate the following integrals:

$$\begin{aligned} \int_0^1 \frac{x^n}{a^2 + (x+y)^2} dx &= \frac{1}{n+1} \left(\frac{1}{a^2 + (1+y)^2} + 2L(n+2) + 2yL(n+1) \right), \\ \int_0^1 \frac{x^n (a^2 - 3(x+y)^2)^2}{(a^2 + (x+y)^2)^3} dx &= 4a^2 (LL(n)(a^2 + y^2) + LL(n+1)2y + LL(n+2)) - 3L(n), \\ \int_0^1 \frac{x^n}{a^2 + (x-y)^2} dx &= \frac{1}{n+1} \left(\frac{1}{a^2 + (1-y)^2} + 2V(n+2) - 2yV(n+1) \right), \\ \int_0^1 \frac{x^n (a^2 - 3(x-y)^2)^2}{(a^2 + (x-y)^2)^3} dx &= 4a^2 (VV(n)(a^2 + y^2) - VV(n+1)2y + VV(n+2)) - 3V(n). \end{aligned} \quad (3.5)$$

Substituting (3.1) into the dual Fredholm equations (2.6) and using (3.5) for integrating the kernels of the Fredholm equations (2.7), we obtain a system of $2N + 3$ equations with the same number of unknowns $F_i, G_i, \tilde{C}_1, i \in [0, N]$:

$$\begin{aligned} \sum_{i=0}^N F_i F_{1ji} + \sum_{i=0}^N G_i G_{1ji} &= 0, \\ \sum_{i=0}^N F_i F_{2ji} + \sum_{i=0}^N G_i G_{2ji} + \tilde{C}_1 &= 0, \\ \sum_{i=0}^N \frac{1}{i+1} G_i &= 0 \quad (0 \leq j \leq N), \end{aligned} \quad (3.6)$$

where F_{kji} and G_{kji} are exact expressions derived with Wolfram Mathematica and depending on β_1 and k .

4. Analysis of the Numerical Results. Let us consider, as an example, two parallel penny-shaped cracks in materials with harmonic potential and with Bartenev–Khazanovich potential (case of equal roots).

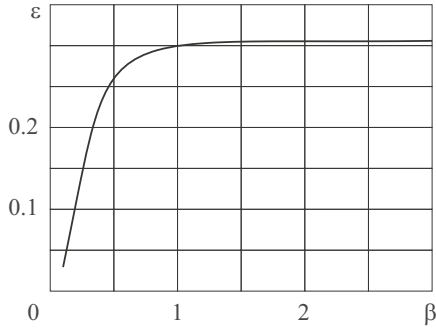


Fig. 2

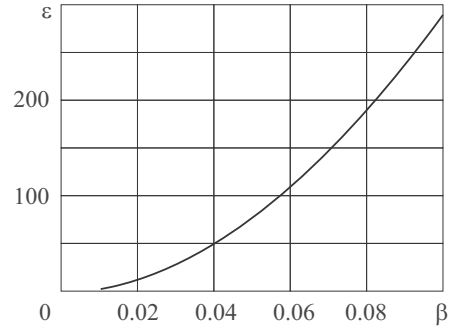


Fig. 3

TABLE 1

β	0.1	0.2	0.3	0.4	0.5	0.6	0.7	0.8	0.9	1.0
$\varepsilon \cdot 10^2$	2.86	9.83	17.54	22.92	25.94	27.63	28.61	29.21	29.60	29.87

4.1. Bartenev–Khazanovich Potential:

$$n_1^0 = n_2^0 = \lambda_1^3, \quad k = (3\lambda_1^3 - 1) / (1 + \lambda_1^3), \quad \beta_1 = 2(n_1^0)^{-1/2} \beta. \quad (4.1)$$

Substituting (4.1) into (3.6), we obtain a system of equations with coefficients F_{kji} and G_{kji} dependent on the parameters β and λ_1 . Analyzing the system of equations (3.6) numerically, we can determine the minimum critical strain ($\varepsilon = 1 - \lambda_1$) and critical stress at which the system loses stability for different values of the dimensionless distance β between the crack and the free surface.

Using 25 coordinate functions, we calculate the function $\varepsilon(\beta)$ (see Table 1 and Fig. 2). These results are in good agreement with the data obtained in [4, 9, 12] which means that the proposed method provides good accuracy.

Using approximate design models for an isolated plane disk-shaped plate under compression, we determined the critical stress $\sigma_{cr} = KD / b^2 a$, where D is a coefficient depending on the material properties; a and b are the thickness and radius of the plate; K is a coefficient depending on the boundary condition of the plate. For clamped boundary conditions and Bartenev–Khazanovich potential, we have $\sigma_{cr} = A_{cr} \beta^2 C_0$, where $A_{cr} = -2.44667$.

Assuming that σ_{11}^0 behaves as $A\beta^2 C_0$ as $\beta \rightarrow 0$, we numerically analyzed the system of equations (3.5) for small values of β . The calculated values of the function $\varepsilon(\beta)$ and the coefficient A are presented in Table 2 and Fig. 3 ($0.01 < \beta < 0.1$).

4.2. Harmonic Potential:

$$n_1^0 = n_2^0 = 1, \quad \lambda_3 = 1 - 2\nu(\lambda_1 - 1) / (1 - \nu),$$

$$k = (\lambda_1(2 - \nu) - (1 - \nu)\lambda_3) / (\nu\lambda_1 + (1 - \nu)\lambda_3). \quad (4.2)$$

Substituting (4.2) into (3.6) and using 20 coordinate functions, as in the case of the Bartenev–Khazanovich potential, we calculate the function $\varepsilon(\beta)$ for different values of Poisson's ratio $\nu = 0.1 \dots 0.5$ (see Table 3 and Figs. 4 ($0.1 < \beta < 3$) and ($0.01 < \beta < 0.1$)).

Table 4 collects the values of the coefficient A obtained on the assumption that $\sigma_{11}^0 \rightarrow A\beta^2 C_0$ as $\beta \rightarrow 0$, and the values of A_{cr} for a clamped penny-shaped plate for different values of Poisson's ratio.

Practical convergence was provided by increasing the number of significant digits to improve the precision of computation.

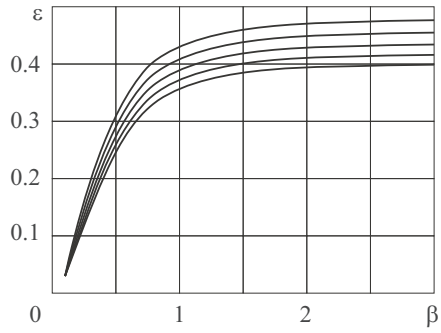


Fig. 4

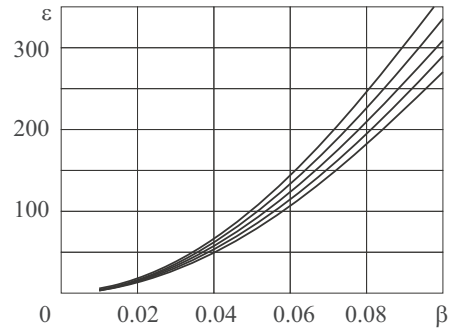


Fig. 5

TABLE 2

β	ε	A
$9 \cdot 10^{-2}$	$2.34269 \cdot 10^{-2}$	-2.32948
$8 \cdot 10^{-2}$	$1.87479 \cdot 10^{-2}$	-2.32564
$7 \cdot 10^{-2}$	$1.45380 \cdot 10^{-2}$	-2.32532
$6 \cdot 10^{-2}$	$1.08187 \cdot 10^{-2}$	-2.32875
$5 \cdot 10^{-2}$	$7.61086 \cdot 10^{-3}$	-2.33624
$4 \cdot 10^{-2}$	$4.93540 \cdot 10^{-3}$	-2.34808
$3 \cdot 10^{-2}$	$2.81367 \cdot 10^{-3}$	-2.36463
$2 \cdot 10^{-2}$	$1.26786 \cdot 10^{-3}$	-2.38630
$1 \cdot 10^{-2}$	$3.21497 \cdot 10^{-4}$	-2.41355
$1 \cdot 10^{-3}$	$3.25751 \cdot 10^{-6}$	-2.44315
$1 \cdot 10^{-4}$	$3.26050 \cdot 10^{-8}$	-2.44537
$1 \cdot 10^{-5}$	$3.25919 \cdot 10^{-10}$	-2.44439
$1 \cdot 10^{-6}$	$3.25854 \cdot 10^{-12}$	-2.44391
$1 \cdot 10^{-7}$	$3.25836 \cdot 10^{-14}$	-2.44377
$1 \cdot 10^{-8}$	$3.25836 \cdot 10^{-16}$	-2.44377
$1 \cdot 10^{-9}$	$3.25833 \cdot 10^{-18}$	-2.44375

TABLE 3

β	ε				
	$\nu = 0.1$	$\nu = 0.2$	$\nu = 0.3$	$\nu = 0.4$	$\nu = 0.5$
1	$4.29445 \cdot 10^{-1}$	$4.08268 \cdot 10^{-1}$	$3.89082 \cdot 10^{-1}$	$3.71619 \cdot 10^{-1}$	$3.55655 \cdot 10^{-1}$
$9 \cdot 10^{-1}$	$4.17705 \cdot 10^{-1}$	$3.96705 \cdot 10^{-1}$	$3.77716 \cdot 10^{-1}$	$3.60461 \cdot 10^{-1}$	$3.44714 \cdot 10^{-1}$
$8 \cdot 10^{-1}$	$4.02108 \cdot 10^{-1}$	$3.81379 \cdot 10^{-1}$	$3.62682 \cdot 10^{-1}$	$3.45733 \cdot 10^{-1}$	$3.30297 \cdot 10^{-1}$
$7 \cdot 10^{-1}$	$3.81157 \cdot 10^{-1}$	$3.60856 \cdot 10^{-1}$	$3.42608 \cdot 10^{-1}$	$3.26117 \cdot 10^{-1}$	$3.11140 \cdot 10^{-1}$
$6 \cdot 10^{-1}$	$3.52772 \cdot 10^{-1}$	$3.33169 \cdot 10^{-1}$	$3.15630 \cdot 10^{-1}$	$2.99845 \cdot 10^{-1}$	$2.85563 \cdot 10^{-1}$
$5 \cdot 10^{-1}$	$3.14203 \cdot 10^{-1}$	$2.95764 \cdot 10^{-1}$	$2.79369 \cdot 10^{-1}$	$2.64696 \cdot 10^{-1}$	$2.51487 \cdot 10^{-1}$
$4 \cdot 10^{-1}$	$2.62267 \cdot 10^{-1}$	$2.45783 \cdot 10^{-1}$	$2.31249 \cdot 10^{-1}$	$2.18338 \cdot 10^{-1}$	$2.06792 \cdot 10^{-1}$
$3 \cdot 10^{-1}$	$1.94673 \cdot 10^{-1}$	$1.81393 \cdot 10^{-1}$	$1.69809 \cdot 10^{-1}$	$1.59615 \cdot 10^{-1}$	$1.50577 \cdot 10^{-1}$
$2 \cdot 10^{-1}$	$1.14100 \cdot 10^{-1}$	$1.05596 \cdot 10^{-1}$	$9.82715 \cdot 10^{-2}$	$9.18973 \cdot 10^{-2}$	$8.62994 \cdot 10^{-2}$
$1 \cdot 10^{-1}$	$3.67084 \cdot 10^{-2}$	$3.37524 \cdot 10^{-2}$	$3.12372 \cdot 10^{-2}$	$2.90707 \cdot 10^{-2}$	$2.71854 \cdot 10^{-2}$
$9 \cdot 10^{-2}$	$3.04124 \cdot 10^{-2}$	$2.79489 \cdot 10^{-2}$	$2.58546 \cdot 10^{-2}$	$2.40522 \cdot 10^{-2}$	$2.24848 \cdot 10^{-2}$
$8 \cdot 10^{-2}$	$2.45623 \cdot 10^{-2}$	$2.25616 \cdot 10^{-2}$	$2.08623 \cdot 10^{-2}$	$1.94011 \cdot 10^{-2}$	$1.81311 \cdot 10^{-2}$
$7 \cdot 10^{-2}$	$1.92093 \cdot 10^{-2}$	$1.76368 \cdot 10^{-2}$	$1.63022 \cdot 10^{-2}$	$1.51554 \cdot 10^{-2}$	$1.41594 \cdot 10^{-2}$
$6 \cdot 10^{-2}$	$1.44057 \cdot 10^{-2}$	$1.32211 \cdot 10^{-2}$	$1.22165 \cdot 10^{-2}$	$1.13538 \cdot 10^{-2}$	$1.06049 \cdot 10^{-2}$
$5 \cdot 10^{-2}$	$1.02036 \cdot 10^{-2}$	$9.36130 \cdot 10^{-3}$	$8.64742 \cdot 10^{-3}$	$8.03471 \cdot 10^{-3}$	$7.50309 \cdot 10^{-3}$
$4 \cdot 10^{-2}$	$6.65540 \cdot 10^{-3}$	$6.10417 \cdot 10^{-3}$	$5.63726 \cdot 10^{-3}$	$5.23671 \cdot 10^{-3}$	$4.88930 \cdot 10^{-3}$
$3 \cdot 10^{-2}$	$3.81219 \cdot 10^{-3}$	$3.49561 \cdot 10^{-3}$	$3.22759 \cdot 10^{-3}$	$2.99774 \cdot 10^{-3}$	$2.79845 \cdot 10^{-3}$
$2 \cdot 10^{-2}$	$1.72383 \cdot 10^{-3}$	$1.58040 \cdot 10^{-3}$	$1.45901 \cdot 10^{-3}$	$1.35494 \cdot 10^{-3}$	$1.26472 \cdot 10^{-3}$
$1 \cdot 10^{-2}$	$4.38077 \cdot 10^{-4}$	$4.01584 \cdot 10^{-4}$	$3.70703 \cdot 10^{-4}$	$3.44235 \cdot 10^{-4}$	$3.21292 \cdot 10^{-4}$
$1 \cdot 10^{-3}$	$4.44205 \cdot 10^{-6}$	$4.07187 \cdot 10^{-6}$	$3.75867 \cdot 10^{-6}$	$3.49017 \cdot 10^{-6}$	$3.25751 \cdot 10^{-6}$
$1 \cdot 10^{-4}$	$4.44617 \cdot 10^{-8}$	$4.07565 \cdot 10^{-8}$	$3.76212 \cdot 10^{-8}$	$3.49341 \cdot 10^{-8}$	$3.26050 \cdot 10^{-8}$
$1 \cdot 10^{-5}$	$4.44437 \cdot 10^{-10}$	$4.07401 \cdot 10^{-10}$	$3.76062 \cdot 10^{-10}$	$3.49200 \cdot 10^{-10}$	$3.25919 \cdot 10^{-10}$
$1 \cdot 10^{-6}$	$4.44345 \cdot 10^{-12}$	$4.07318 \cdot 10^{-12}$	$3.75986 \cdot 10^{-12}$	$3.49127 \cdot 10^{-12}$	$3.25854 \cdot 10^{-12}$
$1 \cdot 10^{-7}$	$4.44324 \cdot 10^{-14}$	$4.07297 \cdot 10^{-14}$	$3.75967 \cdot 10^{-14}$	$3.49112 \cdot 10^{-14}$	$3.25836 \cdot 10^{-14}$
$1 \cdot 10^{-8}$	$4.44321 \cdot 10^{-16}$	$4.07294 \cdot 10^{-16}$	$3.75964 \cdot 10^{-16}$	$3.49109 \cdot 10^{-16}$	$3.25836 \cdot 10^{-16}$
$1 \cdot 10^{-9}$	$4.44321 \cdot 10^{-18}$	$4.07294 \cdot 10^{-18}$	$3.75964 \cdot 10^{-18}$	$3.49109 \cdot 10^{-18}$	$3.25833 \cdot 10^{-18}$

TABLE 4

β	A				
	$A_{cr} = -2.71852$ $\nu = 0.1$	$A_{cr} = -3.05833$ $\nu = 0.2$	$A_{cr} = -3.49524$ $\nu = 0.3$	$A_{cr} = -4.07778$ $\nu = 0.4$	$A_{cr} = -4.89333$ $\nu = 0.5$
$9 \cdot 10^{-2}$	-2.36646	-2.66227	-3.04259	-3.54969	-4.25963
$8 \cdot 10^{-2}$	-2.40442	-2.70497	-3.09139	-3.60662	-4.32795
$7 \cdot 10^{-2}$	-2.44264	-2.74797	-3.14054	-3.66397	-4.39676
$6 \cdot 10^{-2}$	-2.48115	-2.79129	-3.19005	-3.72172	-4.46606
$5 \cdot 10^{-2}$	-2.51994	-2.83493	-3.23992	-3.77990	-4.53588
$4 \cdot 10^{-2}$	-2.55902	-2.87890	-3.29017	-3.83853	-4.60624
$3 \cdot 10^{-2}$	-2.59843	-2.92323	-3.34083	-3.89764	-4.67717
$2 \cdot 10^{-2}$	-2.63817	-2.96795	-3.39194	-3.95726	-4.74871
$1 \cdot 10^{-2}$	-2.67831	-3.01309	-3.44352	-4.01746	-4.82093
$1 \cdot 10^{-3}$	-2.71460	-3.05391	-3.49020	-4.07188	-4.88628
$1 \cdot 10^{-4}$	-2.71710	-3.05674	-3.49339	-4.07564	-4.89075
$1 \cdot 10^{-5}$	-2.71600	-3.05550	-3.49200	-4.07401	-4.88878
$1 \cdot 10^{-6}$	-2.71544	-3.05489	-3.49130	-4.07315	-4.88782
$1 \cdot 10^{-7}$	-2.71531	-3.05473	-3.491130	-4.07297	-4.88754
$1 \cdot 10^{-8}$	-2.71529	-3.05470	-3.491100	-4.07294	-4.88754
$1 \cdot 10^{-9}$	-2.71529	-3.05470	-3.491100	-4.07294	-4.88750

Tables 2 and 4 show that the difference from the results obtained with approximate design models for a clamped circular plate is less than 1% even for $\beta < 0.01$ [1].

The minimum value of β used in the computation is 10^{-9} . The difference between A and A_{cr} does not exceed 0.2%.

Conclusions. We have analyzed, for the first time, the critical parameters defining the fracture of materials compressed along two parallel coaxial penny-shaped cracks for a wide range of distances between the cracks (in the case of equal roots of the characteristic equation). Using the method proposed in [7, 10, 11], we have obtained, for the first time, numerical results for short distances between the cracks (up to $\beta = 10^{-9}$) in materials with harmonic and Bartenev–Khazanovich potentials, which are several orders of magnitude less than those obtained earlier [4, 9, 12].

It has been shown that approximate design models are applicable if the plate isolated by the cracks is thin ($\beta < 0.01$) and is clamped.

REFERENCES

1. A. N. Guz and I. Yu. Babich, *Three-Dimensional Theory of Stability of Rods, Plates, and Shells* [in Russian], Vyscha Shkola, Kyiv (1980).
2. A. N. Guz, *Stability of Elastic Bodies under Triaxial Compression* [in Russian], Naukova Dumka, Kyiv (1979).
3. A. N. Guz, *Brittle Fracture Mechanics of Prestressed Materials* [in Russian], Naukova Dumka, Kyiv (1983).
4. A. N. Guz and V. M. Nazarenko, "Fracture mechanics of material in compression along cracks (review). Highly elastic materials," *Int. Appl. Mech.*, **25**, No. 9, 851–876 (1989).
5. A. N. Guz, *Structural Failure of Materials*, Vol. 1 of the two-volume series *Fundamentals of the Fracture Mechanics of Compressed Composites* [in Russian], Litera, Kyiv (2008).
6. A. N. Guz, *Related Fracture Mechanisms*, Vol. 2 of the two-volume series *Fundamentals of the Fracture Mechanics of Compressed Composites* [in Russian], Litera, Kyiv (2008).
7. A. N. Guz, M. V. Dovzhik, and V. M. Nazarenko, "Fracture of a material compressed along a crack located at a short distance from the free surface," *Int. Appl. Mech.*, **47**, No. 6, 627–635 (2011).
8. A. N. Guz, M. Sh. Dyshel', and V. M. Nazarenko, "Fracture and stability of materials and structural members with cracks: Approaches and results," in: Vol. 5 of the six-volume series *Advances in Mechanics* [in Russian], Litera, Kyiv (2009), pp. 661–705.
9. A. N. Guz, V. I. Knyukh, and V. M. Nazarenko, "Three-dimensional axisymmetric problem of fracture in material with two discoidal cracks under compression along the latter," *Int. Appl. Mech.*, **20**, No. 11, 1003–1012 (1984).
10. M. V. Dovzhik, "Fracture of a half-space compressed along a penny-shaped crack located at a short distance from the surface," *Int. Appl. Mech.*, **48**, No. 3, 294–304 (2012).
11. M. V. Dovzhik, "Fracture of a material compressed along two closely spaced penny-shaped cracks," *Int. Appl. Mech.*, **48**, No. 4, 423–429 (2012).
12. V. I. Knyukh, "Fracture of a material with two disk-shaped cracks in the case of axisymmetric deformation in compression along the cracks," *Int. Appl. Mech.*, **21**, No. 3, 226–231 (1985).
13. V. L. Bogdanov, A. N. Guz, V. M. Nazarenko, "Fracture of a body with a periodic set of coaxial cracks under forces directed along them: An axisymmetric problem," *Int. Appl. Mech.*, **45**, No. 2, 111–124 (2009).
14. A. N. Guz, V. I. Knukh, and V. M. Nazarenko, "Compressive failure of materials with two parallel cracks: Small and large deformation," *Int. Appl. Mech.*, **11**, No. 3, 213–223 (1989).
15. A. N. Guz, "On study of nonclassical problems of fracture and failure mechanics and related mechanism," *Int. Appl. Mech.*, **45**, No. 1, 1–31 (2009).
16. A. N. Guz, I. A. Guz, A. V. Men'shikov, and V. A. Men'shikov, "Penny-shaped crack at the interface between elastic half-spaces under the action of a shear wave," *Int. Appl. Mech.*, **45**, No. 5, 534–539 (2009).
17. I. W. Obreimoff, "The splitting strength of mica," *Proc. Roy. Soc. London*, **127 A**, 290–297 (1930).